

## M87 in hard X-rays: an INTEGRAL view

---

**Sandra De Jong<sup>\*a</sup>, Volker Beckmann<sup>a</sup>, Simona Soldi<sup>b</sup>, Juan A. Zurita Heras<sup>a</sup> & Fabio Mattana<sup>a</sup>**

<sup>a</sup> *François Arago Centre, APC, Université Paris Diderot, CNRS/IN2P3, CEA/Irfu, Observatoire de Paris, Sorbonne Paris Cité, 10 rue Alice Domon et Léonie Duquet, 75205 Paris Cedex 13, France*

<sup>b</sup> *AIM (CEA/DSM-CNRS-Université Paris Diderot) Irfu/Service d'Astrophysique, F-91191 Gif-sur-Yvette, France*

*E-mail: dejong@in2p3.fr*

The nearby FRI radio galaxy M87 is one of the best studied examples of a gamma-ray bright radio galaxy. While in the X-ray band below 10 keV the nucleus of this source shows strong variability, the source does not seem to be detectable in the hard X-ray domain by e.g. Swift or INTEGRAL. Since extrapolating Chandra data indicates that at least during some periods significant hard X-ray emission takes place, we investigate 1.7 Ms effective on-source time of INTEGRAL IBIS/ISGRI data in order to establish the best upper limit in this energy range to date. We have used several techniques to improve the upper limit found, for instance by selecting science windows based on the rms of the significance map. In the energy range 20–60 keV we found an average upper limit of  $< 3.2 \times 10^{-12} \text{ erg cm}^{-2} \text{ s}^{-1}$ . We also analysed other unpublished data from INTEGRAL JEM-X, for which we found a flux of  $1.6 \pm 0.2 \times 10^{-11} \text{ erg cm}^{-2} \text{ s}^{-1}$  between 3–10 keV and an upper limit of  $< 1.2 \times 10^{-11} \text{ erg cm}^{-2} \text{ s}^{-1}$  between 10–25 keV. Together with data from other wavelengths, including Fermi/LAT, we created a spectral energy distribution to investigate the broad-band flux of M87. The upper limit in hard X-rays puts a constraint on the modeling of the overall flux. Since M87 has been detected in the TeV band, combined with the steep power law between hard and soft X-rays, we argue that the SED of M87 might be modeled similarly to a high-peaked BL Lac (HBL), which is a low luminosity blazar.

*An INTEGRAL view of the high-energy sky (the first 10 years) - 9th INTEGRAL Workshop and celebration of the 10th anniversary of the launch*

*15-19 October 2012*

*Bibliothèque Nationale de France, Paris, France*

---

\*Speaker.

## 1. Introduction

Radio galaxies are a subclass of active galactic nuclei (AGN). Radio galaxies have jets and the observer views the jet under a large angle with respect to the line of sight, enabling the view of the core as well as the jet. M87 is a FRI radio galaxy and its jet has an angle of  $30^\circ$  [5]. Due to its proximity,  $D=16$  Mpc [10], it is possible to resolve individual components in the source, such as the core, jet and hotspots in the jet. The central supermassive black hole has an estimated mass of  $M_{\text{bh}}=3\text{--}6 \times 10^9 M_{\text{sun}}$  [9, 7].

M87 has been detected from the radio band up to TeV. Extrapolating from high-flux states observed by Chandra ( $f \sim 2 \times 10^{-12} \text{ erg cm}^{-2} \text{ s}^{-1}$  between 2 and 10 keV) we would expect a flux of  $\sim 10^{-12} \text{ erg cm}^{-2} \text{ s}^{-1}$  in the 20–60 keV band. However, M87 has not been detected at X-rays above  $\sim 10$  keV. Using all available data of M87 with INTEGRAL IBIS/ISGRI we have set an upper limit to the flux in the hard X-ray band using several techniques.

## 2. M87 with INTEGRAL/ISGRI

INTEGRAL/ISGRI has been observing M87 for over 8 years. Using both public and private data we accumulated a total of 1.7 Ms effective on-source time. We have made mosaics between 20–60 keV using the available data with both the Offline Scientific Analysis (OSA) versions 9 and 10. In OSA 10 the reconstruction of the photon energy was improved in several ways, for instance by corrections of the gain and offset drifts<sup>1</sup>.

The first mosaic was made using the standard analysis with OSA 9. Even though the detection significance was  $3.8 \sigma$ , due to the bad image quality we consider the detection not significant. In order to improve the image quality we have created a python routine to judge the quality of the individual science windows. This routine takes the significance extension of the image, creates a histogram of the values and finds the mean and standard deviation from this histogram. The mean value should be 0 and the standard deviation 1, and we put the exclusion limit at 1.2, so science windows with a  $\text{rms} > 1.2$  are omitted ( $\sim 4\%$  of the total). We use a similar technique to quantify the goodness of the mosaic image. A summary of the results of the different techniques can be found in Table 1. In this Table we also give the detection significance of NGC 4388, a bright source ( $f \sim 10^{-10} \text{ erg cm}^{-2} \text{ s}^{-1}$  between 20–60 keV[3]) in the field of M87 as comparison.

Using only the science windows with an  $\text{rms} < 1.2$ , we redo the analysis using OSA 9. The mosaic image improved with this technique, the deviation of the mean of the significance decreased from 1.8 to 1.4, and the detection significance at the source location of M87 drops to  $1.32 \sigma$ , setting the  $3\sigma$  upper limit to  $f < 3.4 \times 10^{-12} \text{ erg cm}^{-2} \text{ s}^{-1}$ . Then we used the same set of science windows and created a mosaic using the new OSA 10 software. This yielded a detection significance at the location of M87 of  $1.35 \sigma$  and an upper limit of  $f < 3.3 \times 10^{-12} \text{ erg cm}^{-2} \text{ s}^{-1}$ .

After this we created mosaics per revolution to judge their quality based on the rms value of the significance map. For the mosaics we set the rms threshold at 1.1, because the fluctuations in the mosaics are more averaged out compared to the single science windows. This can be seen also in Figure 1, where we have plotted the rms of the mosaic per revolution in time, for the mosaics the rms does not exceed 1.2. Our data is spread out over a total of 70 revolutions, and we find

<sup>1</sup>ISDC Newsletter September 2012 <http://www.isdc.unige.ch/newsletter>

that about half of the revolutions have an rms  $> 1.1$ . Most of the revolutions with rms  $< 1.1$  are located in the earlier years of the mission (see Figure 1). We made two separate mosaics of the revolutions with rms  $> 1.1$  and rms  $< 1.1$  to compare the resulting mosaic image and upper limits to the M87 detection. For the mosaic consisting of revolution with rms  $< 1.1$  we found the detection significance for the location of M87 at  $1.7 \sigma$ , and the upper limit is  $f < 4.2 \times 10^{-12} \text{ erg cm}^{-2} \text{ s}^{-1}$  ('selected revolutions' in Table 1). For the mosaic containing the revolutions with the higher rms  $> 1.1$  we found detsig=0 at the location of M87, and we were unable to extract an upper limit flux. In order to increase the detection significance of M87 we have also experimented with some of the parameters concerning ghostbusters, which deals with possible artifacts in the image related to bright sources, and the observation modes, by freezing the position of the dim sources. This was done on a several revolutions, and no improvements were achieved with these techniques.

As a last method we have used a 'border-cutting' technique where we removed the noisy borders of  $\sim 4^\circ$  of the single science windows in order to reduce the noise in the resulting mosaic. The result is a detection significance of  $1.27 \sigma$  and an upper limit of  $f < 3.2 \times 10^{-12} \text{ erg cm}^{-2} \text{ s}^{-1}$  ('borders cut' in in Table 1, significance image in Figure 2).

The  $3\sigma$  upper limit we found of  $f \lesssim 3 \times 10^{-12} \text{ erg cm}^{-2} \text{ s}^{-1}$  is lower than the tentative detection of M87 [11], where a flux of  $f = 8.6 \pm 1.8 \times 10^{-12} \text{ erg cm}^{-2} \text{ s}^{-1}$  in the 20–60 keV band was reported.

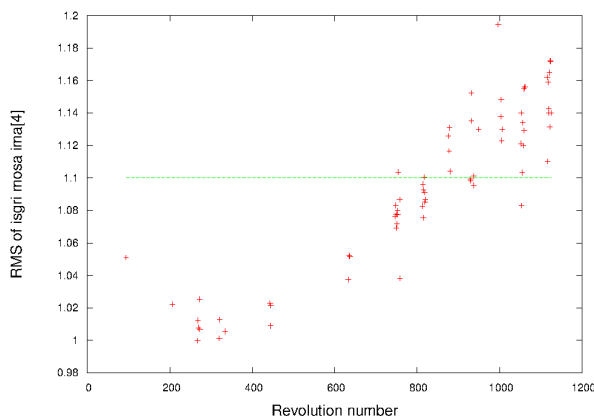


**Figure 1:** The evolution of the rms of the significance of the mosaic per revolution (see text). The line shows the cut for rms=1.1.

### 3. M87 with INTEGRAL/JEM-X

In addition to the INTEGRAL/ISGRI analysis we also extracted images using INTEGRAL/JEM-X. For this we used all available data from 2002 to 2012, with a total exposure time of 440 ks, in two energy bands: 3–10 keV and 10–25 keV. In the energy range 3–10 keV we detect M87 with a significance of  $13 \sigma$  and a flux of  $f = 1.6 \pm 0.2 \times 10^{-11} \text{ erg cm}^{-2} \text{ s}^{-1}$  (Figure 3, left side) in the mosaic of the 2 JEM-X detectors combined. For the 10–25 keV band we did not detect M87, as can also be seen in Figure 3, right side. The upper limit for this range is  $f < 1.2 \times 10^{-11} \text{ erg cm}^{-2} \text{ s}^{-1}$ . Comparing the detection in the 3–10 keV band with the upper limit in the 10–25 keV band requires a power law of with an index  $\Gamma > 2.04$ . Comparing the detection with the ISGRI upper limit

**Table 1:** Results on the derived  $3\sigma$  upper limits of M87 in the 20–60 keV band using the different techniques as described in the text. The upper limit flux is found using mosaic\_spec. We also give the detection significance of the bright source NGC 4388 which is in the field of M87, for comparison.

Method	Mosaic rms	Detection significance M87 [ $\sigma$ ]	count rate [ $s^{-1}$ ]	upper limit [ $\times 10^{-12}$ erg cm $^{-2}$ s $^{-1}$ ]	Detection significance NGC 4388 [ $\sigma$ ]
OSA 9	1.35	1.32	$2.45 \pm 0.02$	3.4	114.1
OSA 10	1.38	1.35	$2.20 \pm 0.02$	3.3	113.5
OSA 10: selected revolutions	1.18	1.70	$2.33 \pm 0.03$	4.2	87.4
OSA 10: borders cut	1.44	1.27	$2.21 \pm 0.02$	3.2	113.2

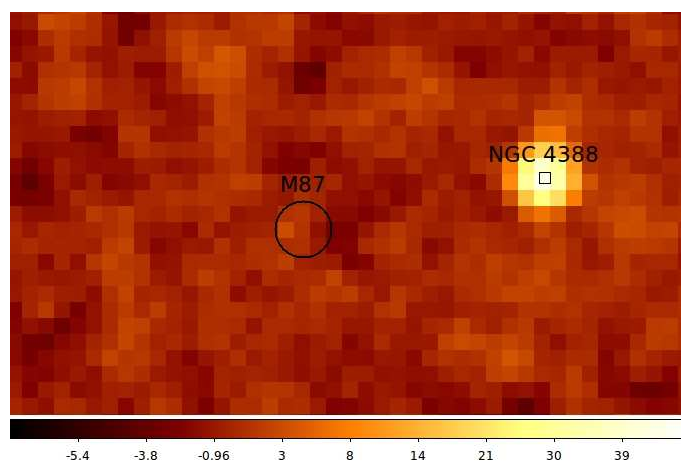


**Figure 2:** ISGRI significance image between 20–60 keV of the M87 region.

requires a steeper power law, with index  $\Gamma > 2.85$ . This can also be seen in the spectral energy distribution in Fig 4, where the JEM-X data points are on the same level in  $\log v f v - \log v$  space, implying a power law with  $\Gamma = 2$ , and the ISGRI upper limit which lies an order of magnitude lower. A power law index of 2.85 is steep compared to other INTEGRAL-detected AGN, in the second INTEGRAL AGN catalogue only 2 out of 22 JEM-X detected sources have a power law index  $> 2.5$  [4].

#### 4. Spectral energy distribution

After deriving the INTEGRAL fluxes we also analysed data from Fermi/LAT from August 2008 to May 2012. In Figure 4 the INTEGRAL fluxes are shown in dark blue, where the inverted triangles are upper limits. The Fermi points are shown in red. To build the spectral energy distribution (SED) we also used historical radio, IR, optical and soft X-ray data of the core of M87 (light blue [1]) and TeV data from HESS (green [2]). Then, we modeled the SED with a one-zone synchrotron self-Compton (SSC) model, a type of model that is often used to model the SED of blazars. The SSC model assumes that the emission from radio to X-ray is produced by synchrotron radiation, emitted by isotropically distributed electrons in a randomly orientated magnetic field of a

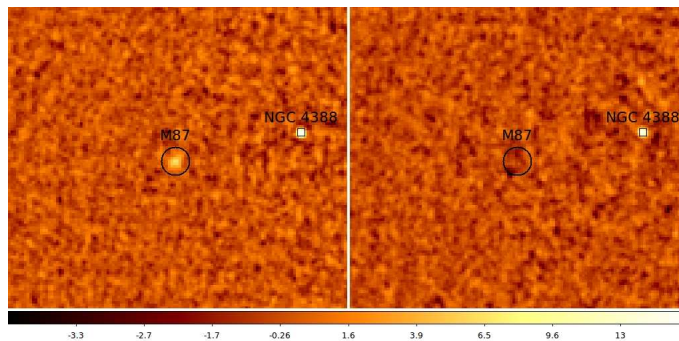


**Figure 3:** JEM-X significance images of the M87 region. Left: the 3–10 keV band,  $f=1.6 \pm 0.2 \times 10^{-11}$  erg cm $^{-2}$  s $^{-1}$ . Right: the 10–25 keV band, upper limit to the flux  $f < 1.2 \times 10^{-11}$  erg cm $^{-2}$  s $^{-1}$

relativistic jet. The electrons are confined in a certain volume, and the electron energy distribution is represented by a broken power law [8]. Then, the synchrotron photons can be seed photons for the inverse Compton scattering on the same electron population as responsible for the synchrotron radiation, which produces the emission from X-rays to TeV. For the modeling of the SED of the core (black line in Figure 4) we used parameters described in [1] and a publicly available code [8]. To reproduce the model we used the Doppler factor of the jet  $\delta=3.9$ , jet angle of  $10^\circ$ , the radius of the emitting volume is  $r = 1.4 \times 10^{16}$  cm and the magnetic field is  $B = 55$  mG. The broken power law that describes the electron energy distribution has a power law index of  $p_1 = 1.6$  between the energies  $E_{\min} = 5 \times 10^5$  keV and  $E_{\text{br}} = 2 \times 10^9$  keV, and the second power law index is  $p_2 = 3.6$  from  $E_{\text{br}} = 2 \times 10^9$  keV to  $E_{\max} = 5 \times 10^{13}$  keV.

The detection and upper limit we derived from the INTEGRAL data lie well above the model of the core. Due to the comparably small distance of M87, it is possible for some instruments (e.g., Chandra, HST) to resolve the spatial structure of the source. M87 spans  $\sim 7'$  by  $7'$  on the sky and the angular resolution of JEM-X is  $3'$  (FWHM), and for ISGRI  $12'$  (FWHM). This implies that for both instruments the observed flux is composed of the core, jet and extended emission, therefore the actual core flux is lower than shown in the SED. Preliminary analysis shows that the actual core flux is lower by a factor of 4, suggesting a core flux deduced from JEM-X data in the order of  $f \sim 4 \times 10^{-12}$  erg cm $^{-2}$  s $^{-1}$ .

## 5. Conclusions and future work

Using several methods, we have set an upper limit to the hard X-ray emission of M87 using all available INTEGRAL/ISGRI data of  $f < 3.2 \times 10^{-12}$  erg cm $^{-2}$  s $^{-1}$  between 20–60 keV. We have also used JEM-X data, which yielded a flux of  $f = 1.6 \pm 0.2 \times 10^{-11}$  erg cm $^{-2}$  s $^{-1}$  between 3 and 10 keV and an upper limit of  $f < 1.2 \times 10^{-11}$  erg cm $^{-2}$  s $^{-1}$  between 10 and 25 keV. The 3–10 flux implies a steep power law with index  $\Gamma > 2.85$  between the soft and hard X-ray band, which can also be seen in the SED.

The fluxes we derived from INTEGRAL do not fit in the SED of the core. Since the derived fluxes are a mixture of core and extended emission (including the jet and diffuse emission) the actual flux of the core is likely to be much lower than the upper limits we derived.

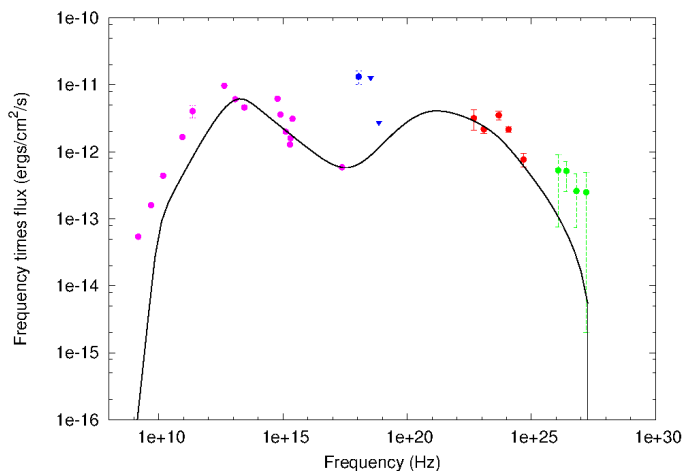


**Figure 4:** Spectral energy distribution of the core of M87. Inverted triangles show upper limits. Dark blue points= INTEGRAL, red=Fermi/LAT, green=HESS [2], light blue=historical radio/IR/optical [1]. The black line shows a SSC model for the core [1].

Next, we want to use another technique to improve the image quality of the INTEGRAL/ISGRI mosaic, and also to improve the upper limit, by using the shadowgrams to create a custom background. The shadowgrams are the sky images as seen through the coded mask, and using the shadowgrams per observation we could possibly reduce the background and increase the detection significance.

For the SED, we will compare the soft X-ray emission of JEM-X with Chandra, in order to disentangle the different contributions. Then, we intend to model the SED with a SSC model with a Compton peak at higher frequency, as is seen in HBL blazars. HBL are a type of blazars with a low luminosity, and the peak frequency of the synchrotron and inverse Compton peaks in the SED are high. These blazars have also a steep power law between the soft and hard X-ray spectrum [6] and are observed at TeV energies, and M87 has both these characteristics.

*This work has been supported by the LabEx UnivEarthS project "Impact of black holes on their environment".*

## References

- [1] A. A. Abdo, M. Ackermann, M. Ajello et al. *ApJ*, 707, 55 (2009)
- [2] F. Aharonian, A. G. Akhperjanian, A. R. Bazer-Bachi et al. *Science*, 314, 1424 (2006)
- [3] V. Beckmann, N. Gehrels, P. Favre et al. *ApJ*, 614, 614 (2004)
- [4] V. Beckmann, S. Soldi, C. Ricci et al. *A&A*, 505, 417 (2009)
- [5] G. V. Bicknell & M.C. Begelman, *ApJ*, 467, 597 (1996)
- [6] D. Donato, R. M. Sambruna & M. Gliozzi, *A&A* 433, 1163 (2005)
- [7] K. Gebhardt & J. Thomas, *ApJ*, 700, 1690 (2009)

- [8] H. Krawczynski, S. B. Hughes , D. Horan et al. ApJ, 601, 151 (2004)
- [9] F. Macchetto, A. Marconi, D. J. Axon et al. ApJ, 489, 579 (1997)
- [10] J. L. Tonry, ApJ, 373, L1 (1991)
- [11] R. Walter & A. Neronov, POS, 7th INTEGRAL workshop (2008)

POS ( INTEGRAL 2012 ) 070